



Flexural Study of Lightweight Concrete Beams casted of

Oil Palm Shell (OPS) Aggregates

Rajasekhar Mekala¹, Sathish Kumar. V²

¹Research Scholar, Department of Civil and Structural Engineering, Annamalai University, India

E-mail: rajasekhar.makala@gmail.com

²Assistant Professor, Department of Civil and Structural Engineering, Annamalai University, India E-mail: aspro_sathish@hotmail.com

Article History	Abstract
<p>Received: 06 Aug 2023 Revised: 05 September 2023 Accepted: 11 November 2023</p> <p>CC License CC-BY-NC-SA4.0</p>	<p><i>This study's main goal is to investigate the potential applications of OPS aggregate in the manufacturing of concrete. This helps to preserve natural resources in addition to addressing the problem of how to get rid of OPS trash. For this study, twelve under-reinforced concrete beams were made and tested. The reinforcing ratios of these beams varied, from 0.52% to 3.90%. The paper presents data related to several important aspects of the beams' behavior, including Information about how the beams deflected under load, Details about when and how cracks formed in the beams, Measures of how much the beams could deform before failure, Information on how the beams rotated at their ends during testing. The flexural behaviour of reinforced OPS concrete beams and other regular reinforced concrete beams was compared in the study. The experimental results and the current industry Codes of practice were found to be reasonably well aligned. Notably, beams with low reinforcement ratios satisfied every serviceability standard listed in BS 8110, proving that they were appropriate for real-world uses.</i></p> <p>Keywords: concrete beams, palm oil, shells, cracks, reinforced behaviour, serviceability</p>

1. Introduction

Presently, Malaysia is the leading global producer of palm oil, with plantations covering more than 4.05 million hectares of land. According to MPOB's 2006 report, these plants yield an exceptional average of approximately 18.88 tonnes of fresh fruit bunches (FFB) per hectare. Large volumes of liquid waste and solid wastes are produced during the grinding of FFB and oil extraction. These waste byproducts include effluent, fiber, shell, and empty fruit bunches. Remarkably, according to Ma et al. (1999), 5.5% of FFB is shell. As a result, an astounding 4 million tonnes of oil palm shell (OPS) solid trash are produced annually. Traditionally, this trash has been burned or occasionally allowed to decompose into big piles, as shown in Figure 1. Such actions endanger the ecology in addition to causing pollution in the environment. Additionally, because of changing environmental restrictions,

disposing of OPS trash has become more expensive. However, OPS waste may be able to be reused as aggregates in recycled aggregate concrete. To be sure, though, further research is necessary. The building industry has found that using OPS waste as a sustainable building material is a workable way to address these environmental and financial issues. This strategy maintains ecological balance while simultaneously protecting natural resources. Furthermore, there is a chance to recycle OPS concrete as aggregates in the creation of recycled aggregate concrete when its useful life comes to an end. The recycling component of OPS concrete construction significantly advances sustainable building practices.

Due to OPS's hard nature and resistance to deterioration, using OPS trash as an environmentally friendly material in the construction sector has emerged as a workable solution to both environmental and financial problems. This strategy maintains ecological balance while simultaneously protecting natural resources. Furthermore, there is a chance to recycle OPS concrete as aggregates in the creation of recycled aggregate concrete when its useful life comes to an end. This recycling component helps to further promote environmentally friendly building methods. concrete, so it doesn't contaminate or leach to create harmful materials (Basri *et al.* 1999). Unlike industrial by-products or artificially produced aggregates, OPS doesn't require any sort of processing or chemical processing to be used efficiently. The bulk density of OPS is between 500 and 600 kg/m³, which leads to concrete that is lightweight with a density of about 1900 kg/m³. Because of this characteristic, OPS concrete is lightweight and has several uses. Studies have shown that OPS concrete may easily reach a compressive strength of more than 17 MPa, satisfying ASTM C330's specification for structural lightweight concrete. According to more recent research, compressive strengths of up to 28 MPa have been found (Teo *et al.*, 2005), suggesting that it may find use in structural applications.

Over the past few decades, the usage of lightweight concrete in the building industry has grown in popularity. Even though a lot of research has been done on the strength characteristics of lightweight aggregate concrete, much of it has focused on aggregates that are produced, naturally occurring, and made from industrial byproducts. OPS concrete has the potential to be used in building applications, which would benefit low-income households as well as the environment since it may be used to build affordable homes, particularly in areas near oil palm fields. The flexural behaviour of OPS concrete beams needs to be thoroughly examined and distinctly determined for structural applications. As a result, the experimental study on the flexural behaviour of reinforced OPS concrete beams is presented in this paper. Researchers looked at the beams' cracking, strength, ductility, and deformation behavior as we gradually loaded them until they failed.

2. OPS and standard granite aggregate comparison

Because OPS aggregates are organic, they have different characteristics from regular granite aggregates, as Table 1 illustrates. OPS aggregates have a high water absorption and a low bulk density capacity due to their porous nature. Because it results in much lighter hardened concrete than traditional granite-based concrete, its low bulk density is desirable. This decrease in a structure's overall dead load results in significant construction cost savings. Furthermore, the resultant concrete's low weight is especially important in earthquake-prone areas. This is because lighter concrete can lessen the destructive forces of inertia that affect structures, which are directly related to the weight of the structure. (Figure 1)



Figure 1 OPS preparation

Studies have indicated that lightweight concretes with high water-absorbing porous aggregates are less susceptible to insufficient curing, particularly in the first phases. This is because the porous lightweight aggregate contains an internal water supply that is stored there (Al-Khaiat and Haque, 1998). Moreover, as compared to granite aggregates, OPS aggregates show notable Aggregate Crushing Value (ACV) and lower Aggregate Impact Value (AIV). In particular, compared to granite aggregates, the AIV and ACV values for OPS were roughly 46% and 58% lower, respectively. This implies that OPS is a highly effective material for absorbing shocks, which increases its appropriateness for a wide range of construction applications.

Materials and mix proportions

OPS aggregates were utilized in place of traditional granite aggregates in the current experiment to create lightweight concrete. Potable water, OPS, river sand, and ordinary Portland cement were the ingredients of the mixture. Table 1 displays the features of OPS that were utilized. Furthermore, the characteristics of granite were also supplied for comparative analysis. The specific gravity, water absorption, and fineness modulus of the river sand were 2.45, 1.40, and 3.89%, respectively. To improve workability, an aqueous Type-F naphthalene sulphonate formaldehyde condensate-based superplasticizer (SP) by ASTM C 494 was added to the mixture. With a water-to-cement ratio of 0.38, each mix contained 1.4 liters for every 100 kg of cement, 848 kg of sand, 510 kg of cement, and 308 kg of OPS.

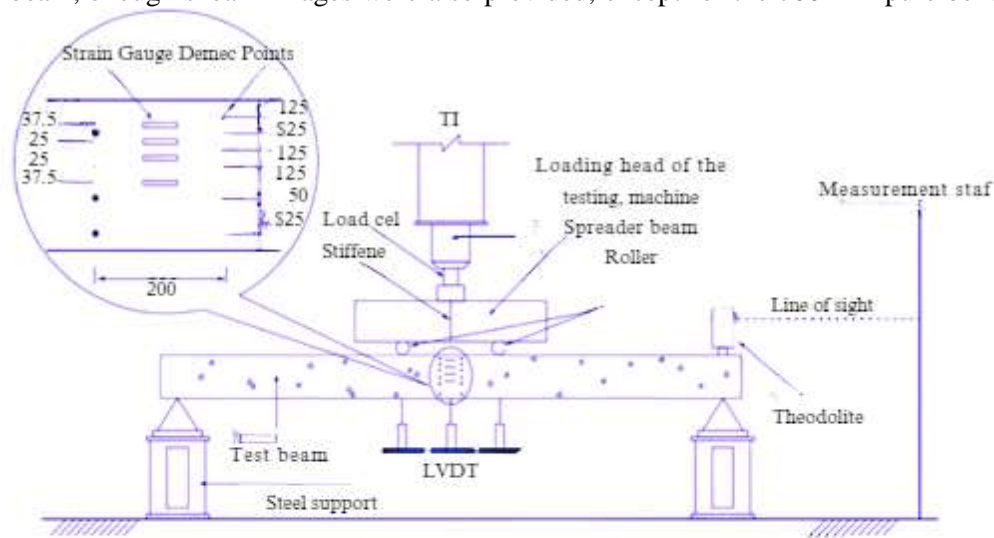
Details of Reinforced concrete beam

Six beams in all were built and put through testing. Under-reinforced beams were the design for the beams. (figure 3) Three beams were strengthened singly (shown as 'S'), while the other three had been reinforced doubly (shown as 'D'). In addition, the necessary quantity of cubes, cylinders, and prisms have been evaluated on the same day as the beam test to ascertain the concrete's qualities. The results are shown in Table 2.

Table 1 Aggregates Properties

Properties	Shell thickness, mm	Bulk density, kg/m ³	Aggregate impact value (AIV), %	Maximum aggregate size, mm	Fineness modulus	Specific gravity (saturated surface dry)	Aggregate crushing value (ACV), %	Los Angeles abrasion value, %	24-hour water absorption, %
Oil Palm Shell (India)	0.1-3	380	21	11	6.1	1.24	12	5.8	25
Granite agg.	-	1490	22	12	6.66	2.59	19	20.3	0.67
OPS agg.	1-2.5	380	18	12	6.08	1.17	8	4.9	28

All of the beams had their breadth (B) and effective depth (d) kept constant at 200 and 150 mm, respectively. The shear span to effective depth ratio of 5.75 meant that the beam sizes and lengths were selected to guarantee that the beams would fail in flexure. Additionally, the beam's proportions were adequate to replicate an actual structural component. Table 3 and Fig. 3 present the beam details. For Y12, Y10, Y20, and Y16, the corresponding yield strengths (fy) were 495, 509, 528, and 510 N/mm². Along the beam, enough shear linkages were also provided, except for the 700 mm pure bending area.



(a) Experimental set-up for the beam specimens

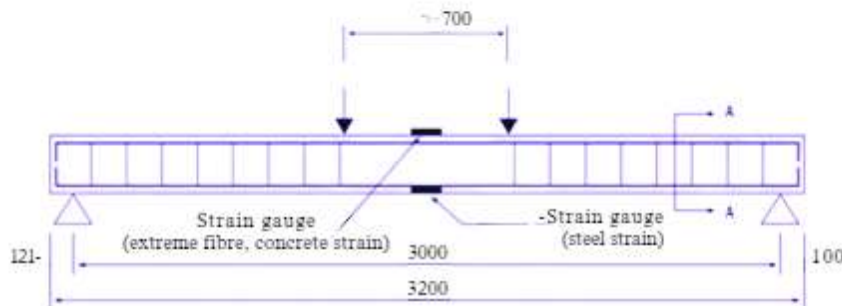


Fig 2 Testing beam details and configuration.

Beam manufacturing, testing, and instrumentation

A 20 mm-long section in the middle of the tension bars was ground smooth to make it easier to attach TML strain gauges (type FLA-10-11). After that, silicone gel was used to seal the area to prevent unintentional damage during concrete pouring. A distinct 20 mm gap was kept between layers of steel bars when more than one layer was needed. When there were various bar sizes involved, the bottom layer was made out of bars with a larger diameter. The beams had been covered with a sheet of plastic and left under a shed (temperature = $28 \pm 5^\circ\text{C}$, relative humidity = 68–91%) as soon as they were cast in wooden molds. The next day, the formwork's sides were peeled, and they were moist-cured for a further six days using wet burlap. Following this, the beams were left in a laboratory environment with $25 \pm 3^\circ\text{C}$ and 74–88% humidity levels until the test's age. Beams were tested when they were between 50 and 60 days old.

- M30 is the grade of concrete utilized.
- OPSC beams are 2000 mm long.
- A 100 mm by 200 mm cross-section of an OPSC beam.
- OPSC beams are strengthened with 8 mm diameter stirrups at 150 mm c/c and 2-10# at the top and bottom.
- Fe500 is the steel grade used.
- Four OPSC beams, designated as CB1, CB2, CB 3, and CB 4, were cast for testing under both cyclic and monotonic load scenarios.

To quantify the strains at various depths before testing, Demec points (model: PL-60-11) and TML strain gauges were fastened to the concrete substrate in the middle region of the beams, as shown in Fig. 4. A strain gauge was also used to measure the compressive strains in the pure bending zone of the concrete on the upper surface of the beams. Two LVDTs (linear voltage displacement transducers) were employed to measure the deflections immediately below the loading sites and one at the midspan. Every strain gauge and LVDT was linked to a portable data recorder, from which a computer recorded the values at predetermined load intervals until the beam failed.

- The middle third region of the beams had the highest deflection under monotonic loading when they were tested under symmetrical loading.
- The beams were evaluated until they broke.
- Flexural fissures began to form and spread towards the point of loading as the load rose, causing the beam to deflect.
- In the middle of the region of continuous bending moment, failure took place in a typical flexure mode.
- The maximum bending moment is carried by the reinforcement in the tensile zone, which rotates the beam. More flexural cracks were found to be vertically extended upward and to have a wider width.



Fig. 3 Beam testing four-point load. details.

A theodolite with a one-second precision was used to measure the beams' terminal revolutions. To record vertical readings at each load increment, (table 2)a measuring staff member was set up at a distance from the theodolite, which was precisely placed on the beam over the bearing point (Fig. 4).

Table 2 Properties of OPS concrete.

Beam type	Air-dry density (kg/m ³)	Elastic modulus (GPa)	Modulus of rupture (map)	Compressive strength (MPa)	Split tensile strength(MPa)
Doubly reinforced	1940	5.05	4.89	25.3	1.67
Singly reinforced	1965	5.28	4.93	26.3	1.82

As seen in Fig. 5, the test was conducted with a 1,000 kN hydraulic actuator, subjecting the beams to two-point forces in a load monitoring mode with increments of 15 to 25 until failure. (table 3)

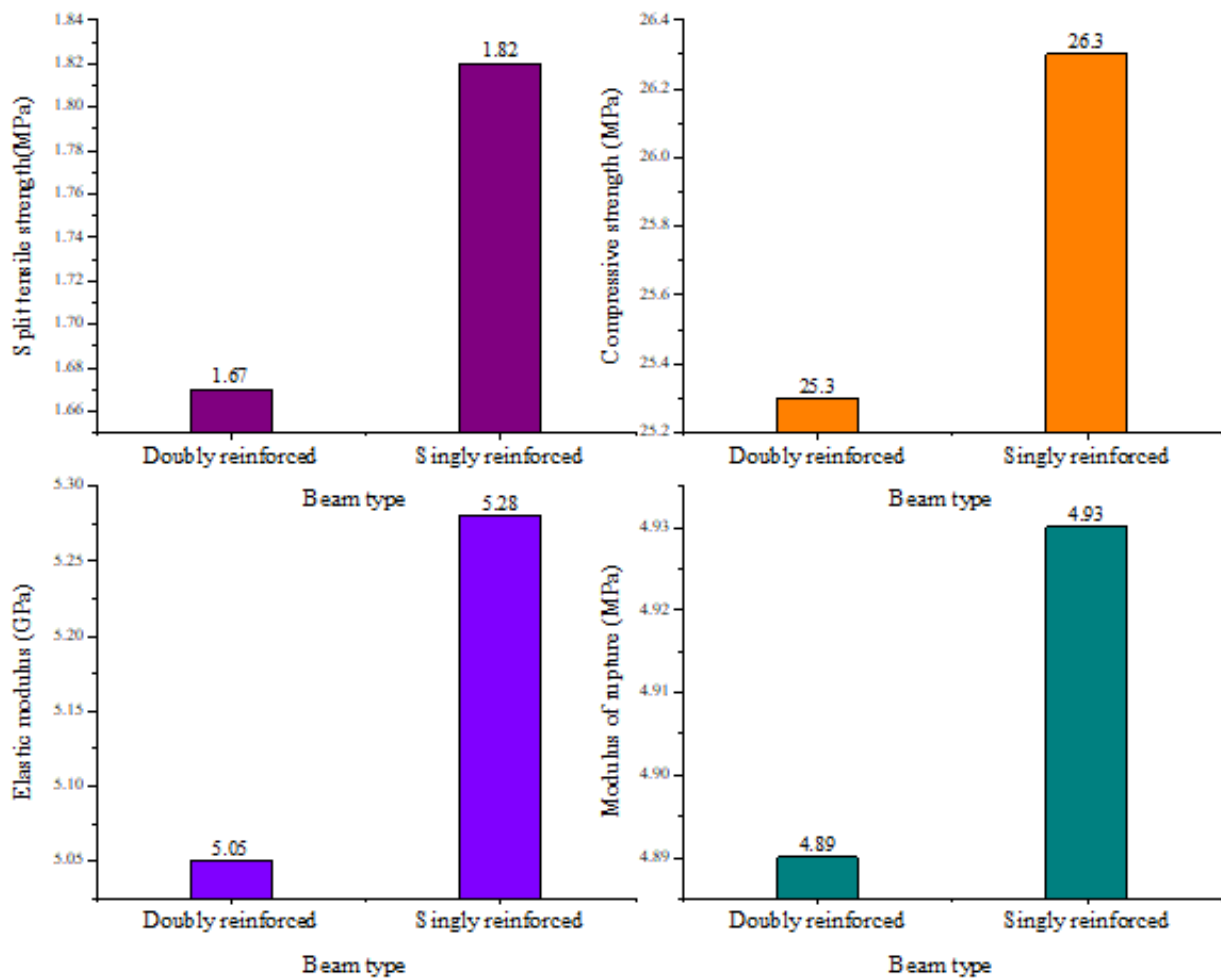


Fig 4 Graph of beam type reinforcement (both singly and doubly)

Table 3 Test beam details.

Beam type	Doubly	Doubly	Doubly	Single	Single	Single
Nominal / compression reinforcement no. and size	2Y10	2Y16 + 1Y12	2Y20 + 1Y10		2R8	
Tension reinforcement number & size	3Y16	3Y20	3Y20 + 2Y12	2Y10	2Y12	3Y12
Area of tensile steel, A_s (mm^2)	603	943	1169	157	226	339
Beam size, B x D (mm)	150 x233	150 x235	150 x242	150 x230	150 x231	150 x231
$\rho = A_s/b d, \%$	2.01	3.14	3.9	0.52	0.75	1.13
Beam no	D1	D2	D3	S1	S2	S3

Figure 6 shows the area tensile strength. When compared to traditional aggregates, the majority of lightweight aggregates—including OPS—generally have greater water absorption ratings. Figure 7 deals with the concrete structure. While OPS has an elevated water absorption rate, other aggregates, such as pumice, have even higher rates of absorption (about 37%; Hossain, 2004). On the other hand, the high water retention of OPS aggregates may be beneficial for the hardened concrete that results. Fig 8. Shows the static test on a controlled beam

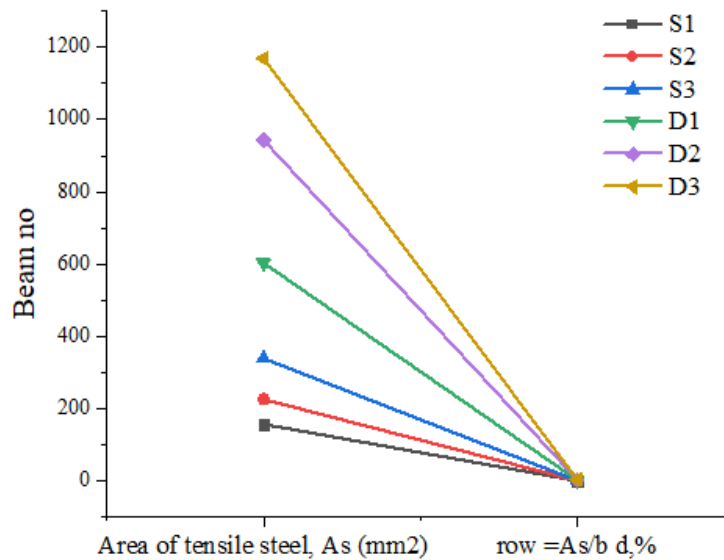


Fig. 5 Graph of tensile steel area



Fig. 6 Beam crack patterns.

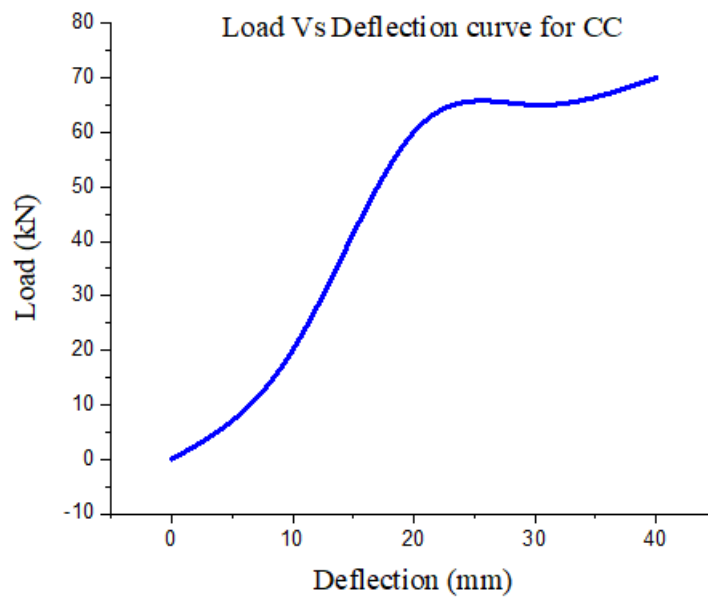


Fig. 7 Static test on controlled beam

4. Results and discussions

General observations

In flexure, every beam exhibited normal structural behavior. Bond failure can happen during testing because the OPS aggregates' concave and convex surfaces are smooth. On the other hand, no horizontal cracks were seen at the reinforcing level, indicating that bond failure had not occurred. The constant-moment zone showed signs of vertical flexural cracks, and the compression concrete's crushing with a large amount of final deflection caused the eventual failure. Because every beam had insufficient reinforcement, the tensile reinforcement gave way before the concrete surface in the pure bending zone was crushed. The covering of concrete on the area of compression began to spill as soon as the maximum force was applied. Ultimately, during failure, the concrete cover was crushed. The concrete's crushing depth ranged from 60 to 120 mm at failure.

Bending moments

Table 4 displays a comparison of the theoretical design moments and the experimental ultimate moments (Mult). Per the recommendation of BS 8110, the rectangular stress block analysis was used to forecast the projected design moment (Mdes) of the beams. The ultimate moment from the experiment was between 4% and 35% greater than the projected values for beams with a ratio of reinforcement of

3.14% or less. However, the simulated ultimate moment was around 6% lower for high reinforcement ratios, i.e., at 3.9%. According to the results of the testing, BS 8110 can be utilized for OPS concrete beams to offer a sufficient load factor against failure and an optimistic estimation of the final breaking capacity for ratios of reinforcement up to 3.14%.

Deflection behavior

The typical test moment-deflection curves for the single- and double-reinforced beams are displayed in Figures 9 and 10, respectively. The moment-deflection curve in all beams had a sharp, nearly linear slope before cracking. The moment-deflection curve showed a shift in slope as soon as flexural cracks appeared, and this slope persisted linearly until the steel reinforcement began to yield. (table 4) It is evident from the bending curves that OPS concrete beams behave similarly to other lightweight cement beams. (Swamy and Ibrahim 1975; Swamy and Lambert 1984).

Table 5 presents a comparison between the experimental data and the projected midspan displacement under service moments. Using the formula, the expected deflection is computed based on the beam curvatures by BS 8110.

Table 4 Comparison of ultimate moments in theory and experiment.

Theoretical design moment, Mdes, (kNm)	(3)	42.46	73.87	89.09	13.6	18.07	24.73
Experimental ultimate moment, Mult (kNm)	(2)	50.03	77.05	83.38	16.1	22.14	33.35
Capacity ratio of OPS Concrete beams (2)/(3)	(4)	1.18	1.04	0.94	1.23	1.17	1.35
Neutral axis depth at Ultimate moment (mm)	(1)	137.01	140.18	155.3	50.03	67.2	81.12
Beam no		D1	D2	D3	S1	S2	S3

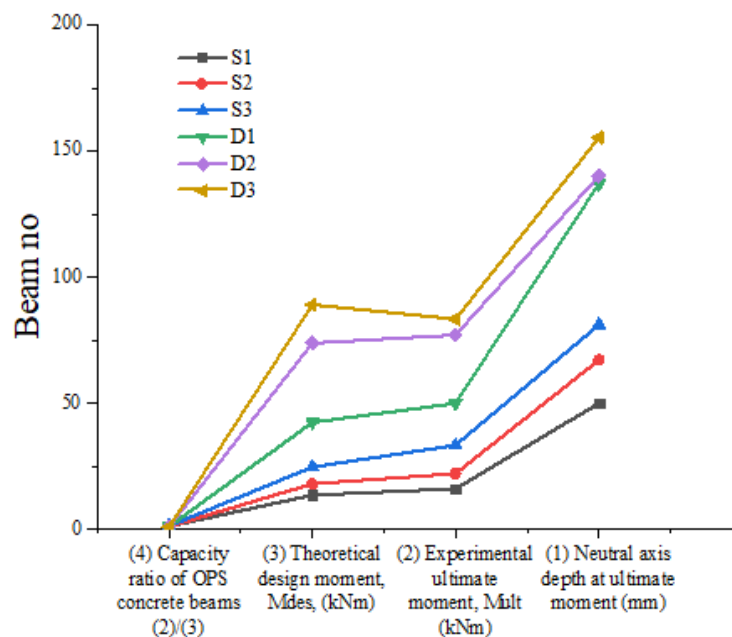


Fig. 8 Four analysis of oil palm shell with concrete

Table 5 OPS concrete beam deflection during service.

Theoretical design service moment, Ms(kNm)	26.709	46.322	55.614	8.654	11.454	15.611
$\Delta_{exp}/\Delta_{the o}$	0.96	1.12	1.21	1.06	0.92	0.86
Span/Δ_{exp}.	196	146	159	263	256	252
Theoretical deflection, $\Delta_{the o}$, BS8110(mm)	15.9	18.35	15.5	10.75	12.76	13.9
Deflection from experiment, Δ_{exp}(mm)	15.3	20.5	18.8	11.4	11.7	11.9
Beam no.	D1	D2	D3	S1	S2	S3

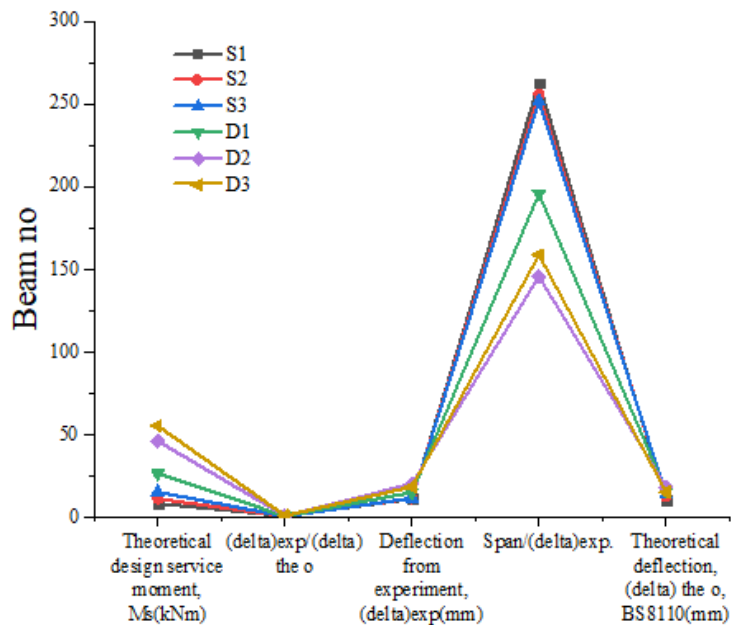


Fig. 9 Deflection behaviour of 4 ultimate designs

Ductility behavior

A member must be able to withstand significant deflections at almost maximum load-carrying capacity for reinforced concrete structures to be ductile and to give sufficient warning of impending failure. The displacement ductility was examined in this work. The tested OPS concrete beams' ductility is displayed in Table 6. High ductility ratios often mean that a structural element can experience significant deflections before failing. This study found that the ductility ratio was greater than 3 for beams with reinforcement ratios up to 2.01%, indicating rather excellent ductility. The OPS aggregates' toughness and good shock absorption qualities, as shown by Table 1's aggregate crushing value (ACV) and aggregate impact value (AIV), were among the elements influencing the OPS beams' good ductility behavior. (figure 11) According to Ashour (2000), structural elements that are subjected to significant displacements, including rapid stresses brought on by earthquakes, can be considered if their displacement ductility falls between 3 and 5. This experiment also revealed that less ductile behavior is produced by a higher tension augmentation ratio. This is consistent with previous studies' findings. (Lee and Pan 2003; Rashid and Mansur 2005).

Table 6 Experimentally determined displacement ductility of OPS concrete beams.

Displacement ductility ratio	Δ_u/Δ_y	3.14	2.65	2.49	4.34	4.34	4.2	3.55
Yield stage	Moment, kNm	37.375	63.25	69	11.5	11.5	15.813	25.875
	Deflection, Δ_y (mm)	23.34	29.56	24.4	16.64	16.64	17.48	21.72
Ultimate Stage	Moment, kNm	50.025	77.05	83.375	16.1	16.1	22.138	33.35
	Deflection, Δ_u (mm)	73.26	78.38	60.76	72.18	72.18	73.4	77.2
Beam no		S1	D1	D2	D3	S1	S2	S3

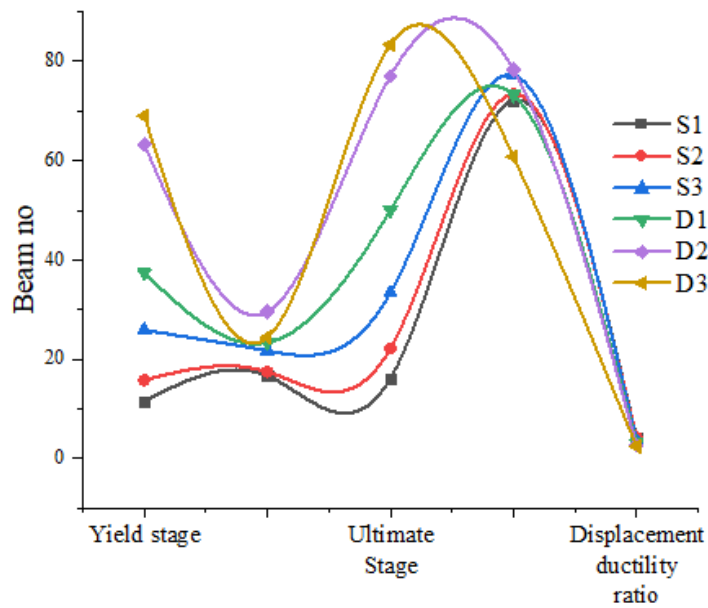


Fig. 10 Ductility behaviour

Cracking behavior

At the tension steel level, crack widths were recorded at each load interval, and the crack forms were recorded on the beam. Initial cracking developed at roughly 5 to 9% of the ultimate load for the doubly reinforced beams and at approximately 11 to 15% of the ultimate load for the singly reinforced portions. (figure 12) This indicates that the first crack happens at a lower proportion of the ultimate stress with larger reinforcing ratios. It was observed that the initial crack consistently manifests itself in proximity to the beam's midspan. The majority of the cracks that were developing on the beams' surface were vertical, indicating flexural failure. Table 7 shows the cracking features of OPS concrete beams.



Fig.11 Concrete TOPS beam crack behavior

Using the formula suggested by ACI 318, the theoretical cracking moment ($M_{CR}(\text{theo})$) of the beam is calculated, approximating the empirical cracking moments. Therefore, to more accurately anticipate the cracking moment, a decreased value of roughly 55% of f_r must be employed.

Table 8 also presents a comparison between the experimental values and the expected crack width based on BS 8110 and ACI 318 under service loads. It was noted that the fracture width predictions provided by the ACI 318 and BS 8110 codes were fairly accurate. However, compared to BS 8110, ACI 318 more accurately forecasts the experimental fracture widths of OPS beams. The maximum permitted crack widths, as stated in the majority of codes of practice, vary from 0.10 to roughly 0.40 mm, contingent on the exposure circumstances. Crack widths up to 0.41 mm are allowed by ACI 318 for members that are weather-protected. OPS concrete was found to have fracture widths at service load that were less than those of the maximum lightweight aggregate concrete composed of expanded shale (Aglite) and expanded slate (Solite). (Swamy and Ibra- him 1975).

End rotation

Figs. 13 and 14 show the moment-end rotation profiles of OPS concrete beams. The curvature of a beam is affected by the end rotations.

Table 7 Features of OPS crack concrete beams.

Average crack spacing, (mm)	99	92	80	107	77	90
Experimental crack wid that failure (mm)	1.1	1	0.8	1.24	0.9	0.82
Experimental crack wid that M_s (mm)	0.26	0.26	0.27	0.22	0.22	0.22
Experimental cracking moment, M_{CR} (exp) (kNm)	4.313	4.313	5.75	2.3	2.875	3.738
Number of cracks between loading points	8	7	10	6	8	8
Theoretical cracking moment - M_{CR} (the o) (kNm)	6.637	6.751	7.159	6.52	6.577	6.577
design service moment - M_s (kNm)	26.71	45.132	55.85	8.65	10.385	16.19
Beam no	D1	D2	D3	S1	S2	S3

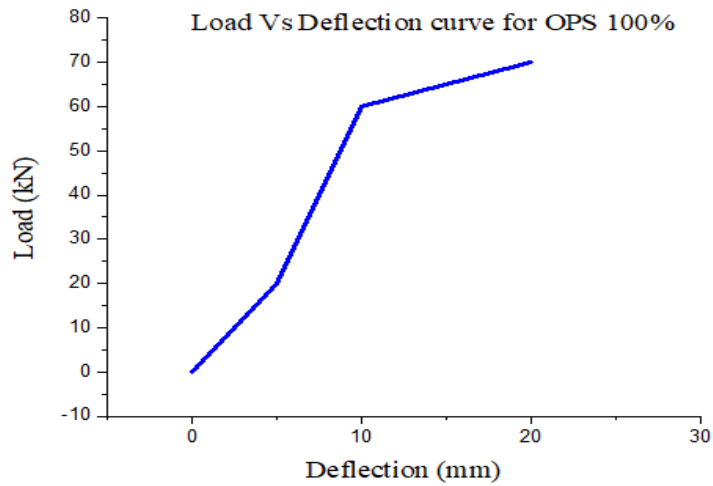


Fig. 12 Deflection level of OPS concrete

Table 8 contrasts the experimental and projected crack widths at service loads.

(2) / (4)	0.23	0.3	0.37	0.19	0.19	0.19
(2) / (3)	0.26	0.26	0.27	0.22	0.22	0.22
Experimental crack width(mm)	0.19	0.23	0.23	0.23	0.22	0.22
Theoretical crack widths, ACI(mm)	1.13	0.87	0.73	1.16	1.16	1.16
Theoretical crack widths, BS8110(mm)	1.37	1.13	1.17	0.96	1	1
Beam no	D1	D2	D3	S1	S2	S3

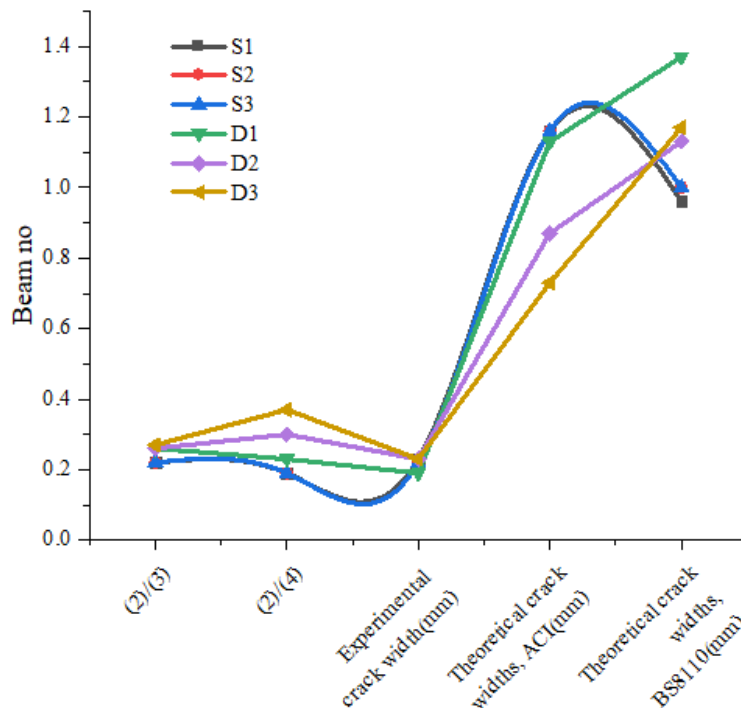


Fig. 13 Strain distributions during loading.

It is evident from the figure that the moment-end rotation curve's shape resembles the typical moment-curvature curve behavior, (figure 15) increasing linearly until steel yielding occurs. After yielding, the moment increased very little but the end rotations increased quickly. The final rotation of the beams before the collapse was seen to range from $3^{\circ} 3' 9.79''$ to $3^{\circ} 20' 19.83''$, which is similar to other lightweight concretes. (Swamy and Lambert 1984).

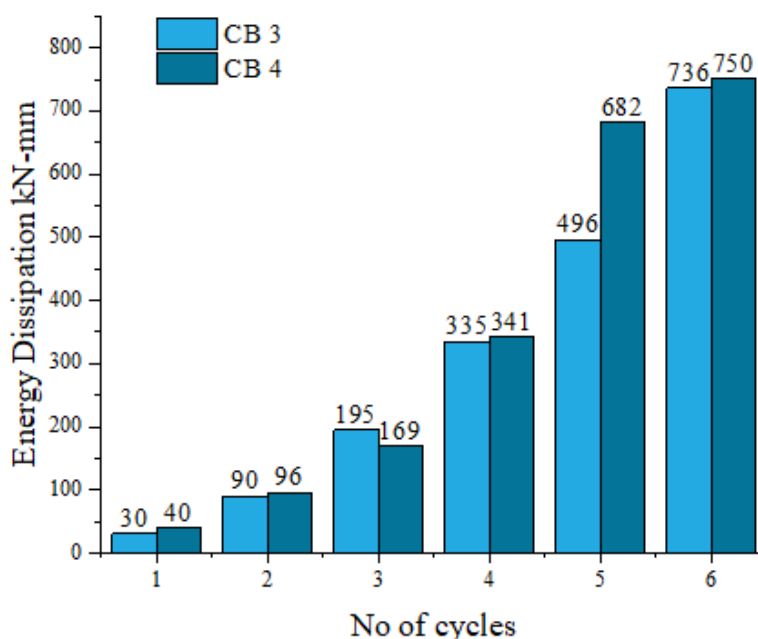


Fig. 14 Energy dissipation phase

Concrete and steel strains

At each load increase, the strains in the steel and concrete were determined. Fig. 15 shows the strain pattern for the steel and concrete. The concrete's compressive stresses varied from 498 to 1303 $\times 10^{-6}$ under service loads. Just before failure, the measured strains in the steel and concrete were 2093 to 6069 $\times 10^{-6}$ and 2105 to 5480 $\times 10^{-6}$, respectively. However, it should be noted that the strain measurements were obtained at roughly 95% of the failure load; as a result, the real strain values are significantly higher than those presented here. However, the results obtained are in line with those of other studies. (Swamy and Ibrahim 1975; Swamy and Lambert 1984). These findings further demonstrate that, when subjected to flexural loadings, OPS concrete can reach its maximum strain capacity.

5. Conclusions

According to the outcomes of the experimental study, OPS concrete's flexural behaviour is generally similar to that of other lightweight concrete types. This suggests that OPS can be used as coarse aggregate in the creation of structural lightweight concrete, particularly for the building of affordable homes. The current findings from experiments allow for the following findings and deductions.

- (1) The flexure of all OPS concrete beams displayed typical structural behaviour. Because the beams were under reinforced, the pure bending zone's tensile reinforcement yielded before the compression concrete was crushed.
- (2) Experimental ultimate moments were found to be between 4% and 35% greater than the projected moments, while the ultimate moments predicted using BS 8110 offer a cautious estimate for OPS concrete beams up to a strengthening ratio of 3.14%. The ultimate moment capacity for the beam with a 3.90% reinforcement ratio is approximately 6% less than what BS 8110 states.
- (3) Reasonable forecasts can be made using the OPS concrete deflections under service loads, which were computed using BS 8110. For the individually reinforced beams, the deflection under the design load conditions was within the permissible limit given by BS 8110. The deflections at service forces for the doubly strengthened beams were greater than the allowable limits, indicating that the beam levels ought to be raised.
- (4) The ductility behaviour of the OPS concrete beams was good. Every beam showed a significant degree of deflection, giving adequate notice of the impending failure.
- (5) The crack widths at service loads were within the maximum value permitted by BS 8110 for durability standards, ranging from 0.22 mm to 0.27 mm.

References

- ACI 318, (1995). “*Building code requirements for reinforced concrete.*” Detroit: American Concrete Institute.
- Al-Khaiat, H. and Haque, M. N. (1998). “Effect of initial curing in early strength and physical properties of a lightweight concrete.” *Cement and Concrete Research*, 28(6), 859-866.
- Ashour, S. A. (2000). “Effect of compressive strength and tensile reinforcement ratio on flexural behaviour of high-strength concrete beams.” *Engineering Structures*, 22(5), 413-423.
- ASTM C 330. *Standard specification for lightweight aggregates for structural concrete.* Annual Book of ASTM Standards.
- ASTM C 494. *Standard Specification for Chemical Admixtures for Concrete.* Annual Book of ASTM Standards.
- Basri, H. B., Mannan, M. A. and Zain, M. F. M. (1999). “Concrete using waste oil palm shells as aggregate.” *Cement and Concrete Research*, 29(4), 619-622.
- BS 8110, (1985). “*Structural use of Concrete Part 1. Code of Practice for Design and Construction.*”, London: British Standard Institution.
- Güdüz, L. and Uğur, İ. (2005). “The effects of different fine and coarse pumice aggregate/cement ratios on the structural concrete properties without using any admixtures.” *Cement and Concrete Research*, 35(9), 1859-1864.
- Hossain, K. M. A. (2004). “Properties of volcanic pumice based cement and lightweight concrete.” *Cement and Concrete Research*, 34(2), 283-291.
- Lee, T. K. and Pan, A. D. E. (2003). “Estimating the relationship between tension reinforcement and ductility of reinforced concrete beam sections.” *Engineering Structures*, 25(8), 1057-1067.
- Ma, A. N., Toh, T. S. and Chua, N. S. (1999). “Renewable energy from oil palm industry.” In: Singh G., Lim K. H., Teo L. and Lee D. K., *Oil palm and the Environment: A Malaysian Perspective*, Malaysian Oil Palm Growers’ Council, Kuala Lumpur, Malaysia, 253-259.
- Malaysian Palm Oil Board (MPOB) 2006. “A summary on the performance of the Malaysian oil palm industry – 2005 [online].” Available from: http://econ.mpob.gov.my/economy/summary_latest05.htm [Assessed on 5 July 2006].
- Mannan, M. A. and Ganapathy, C. (2004). “Concrete from an agricultural waste-oil palm shell (OPS).” *Building and Environment*, 39(4), 441-448.
- Rashid, M. A. and Mansur, M. A. (2005). “Reinforced high-strength concrete beams in flexure.” *ACI Structural Journal*, 102(3), 462-471.
- Swamy, R. N. and Ibrahim, A. B. (1975). “Flexural behaviour of reinforced and prestressed Solite structural lightweight concrete beams.” *Building Science*, 10(1), 43-56.
- Swamy, R. N. and Lambert, G. H. (1984). “Flexural behaviour of reinforced concrete beams made with fly ash coarse aggregates.” *The International Journal of Cement Composites and Lightweight Concrete*, 6(3), 189-200.
- Teo, D. C. L., Mannan, M. A., Kurian, V. J. and Ganapathy, C. (2006). “Lightweight concrete made from oil palm shell (OPS): Structural bond and durability properties.” *Building and Environment*, In Press, DOI: 10.1016/j.buildenv.2006.06.013.
- Teo, D. C. L., Mannan, M. A. and Kurian, V. J. (2005). “Structural performance of lightweight concrete.” In: *Conference on Sustainable Building Southeast Asia*, Kuala Lumpur 11-13 April 2005, 254-258.